

---

1 This manuscript has been submitted for publication to Geochemical Perspectives Letters on  
2 November 16<sup>th</sup>, 2023. Please note that this manuscript has not undergone peer review, nor  
3 has it been formally accepted for publication. Subsequent versions of this manuscript may  
4 have slightly different content. Feel free to reach out the corresponding author. We  
5 welcome constructive feedback.

---

## 7 Reykjanes Peninsula's historical eruptions: SO<sub>2</sub> emissions and 8 future hazard implications

9 A. Caracciolo<sup>1</sup>, E. Bali<sup>1</sup>, E. Ranta<sup>2</sup>, S. A. Halldórsson<sup>1</sup>, G. H. Guðfinnsson<sup>1</sup>

10

11 (1) NordVulk, Institute of Earth Sciences, University of Iceland, 102, Reykjavík, Iceland.

12 (2) Department of Geosciences and Geography, University of Helsinki, Finland

13

14

15 Corresponding author: Alberto Caracciolo ([alberto@hi.is](mailto:alberto@hi.is))

16

17

18

19

20

21

22

23

24

25

26

27

28

29

30

31

## 32 Abstract

33 Exposure to volcanic SO<sub>2</sub> can have adverse effects on human health, with severe respiratory disorders  
34 documented on the short- and long-term timescale. Here, we use melt inclusion (MI) and groundmass  
35 glass data to calculate syn-eruptive SO<sub>2</sub> emission potentials across the Reykjanes peninsula (RP), the  
36 most populated area of Iceland that has recently undergone magmatic reactivation with the 2021,  
37 2022, 2023 AD Fagradalsfjall eruptions. We target 16 individual eruptions from the previous volcanic  
38 episode at the RP, the 800-1240 AD Fires. Geochemical modelling indicates that pre-eruptive variability  
39 in sulfur contents can be explained by fractional crystallization and mixing of geochemically diverse  
40 mantle-derived melts. We calculate SO<sub>2</sub> emission potential across the RP to be in the range 0.004-7.4  
41 Mt. These estimates correspond to daily SO<sub>2</sub> emissions in the range 600-53000 tons/day, higher than  
42 the mean SO<sub>2</sub> field measurements of 5240 ± 2700 tons/day during the 2021 AD Fagradalsfjall eruption.  
43 By using maximum and minimum sulfur values preserved in undegassed MIs, we develop an empirical  
44 approach to calculate best- and worst-case SO<sub>2</sub> emission potential scenarios of any past or ongoing RP  
45 eruption of known effusion rate. We conclude that the potential sulfur emissions across the RP can be  
46 significantly higher than observed during the 2021 AD Fagradalsfjall eruption, mainly because of the  
47 more evolved nature and higher sulfur contents of magmas erupted during the 800-1240 AD Fires.  
48 Based on dominant wind directions on the RP, eruptions in Brennisteinsfjöll pose the greatest health  
49 hazard to the capital area. Our findings enable assessing of SO<sub>2</sub> emission scenarios of future eruptions  
50 across the RP and can be used together with gas dispersal models to forecast SO<sub>2</sub> pollution at ground  
51 level and its impact on human health.

52

53

## 54 Introduction

55 The release of volcanic gases and aerosols during volcanic eruptions can significantly impact the air  
56 quality and climate (e.g. Ilyinskaya *et al.*, 2017; Milford *et al.*, 2023), as well as the biodiversity (e.g.,  
57 Weiser *et al.*, 2022). Among volcanic gases, sulfur species (SO<sub>2</sub>, H<sub>2</sub>S) and associated aerosols (SO<sub>4</sub>,  
58 H<sub>2</sub>SO<sub>4</sub>) are the most critical aerial hazard for human health, with short and long-term impacts that  
59 have been recorded at variable distances from eruptive vents (e.g., Ilyinskaya *et al.*, 2017; Schmidt *et al.*,  
60 2015). For example, several studies have associated cardiorespiratory health issues with volcanic  
61 sulfur emissions (e.g., Carlsen *et al.*, 2021; Heaviside *et al.*, 2021). Hence, a detailed knowledge of  
62 sulfur release potential of active volcanoes located in densely populated areas is critical to understand  
63 air quality hazards of future volcanic eruptions. This is the case of the Reykjanes peninsula (RP) in  
64 southwest Iceland, an active spreading area segmented into five volcanic systems that hosts ~70% of  
65 the Icelandic population. The latest magmatic period in the RP occurred ~800 years ago (Sæmundsson

66 et al., 2020) but knowledge about sulfur outputs during those eruptions has been lacking thus far. Each  
67 volcanic systems on the RP tend to activate during individual magmatic periods (Sæmundsson et al.,  
68 2020) and the recent 2021, 2022 and 2023 AD Fagradalsfjall eruptions (Barsotti et al., 2023; Einarsson  
69 et al., 2023) suggest the potential initiation of a new magmatic period. Consequently, there is an  
70 increased societal need for a deeper understanding of sulfur emissions across the RP. This is crucial for  
71 a comprehensive assessment of sulfur's impact during future eruptions across the RP and its potential  
72 consequences for human health.

73 In this study, we calculate syn-eruptive sulfur release and sulfur emission potential of 16 geologically  
74 and petrochemically well characterized magmatic units erupted in the volcanic systems of Reykjanes,  
75 Svartsengi, Krýsuvík and Brennisteinsfjöll during the 800-1240 AD Fires (Caracciolo et al., 2023;  
76 Halldórsson et al., 2022; Peate et al., 2009) and compare those with sulfur emissions from 2021 AD  
77 Fagradalsfjall eruption (Barsotti et al., 2023; Halldórsson et al., 2022). Also, we estimate daily SO<sub>2</sub>  
78 emissions for the 800-1240 AD Fires and develop an empirical approach to calculate worst- and best-  
79 case sulfur emission potentials for any eruption of a given volume emplaced in the RP.

## 80 Samples and methods

81 Samples consist of scoria collected from multiple vents within individual eruptive units erupted during  
82 the 800-1240 AD Fires (Caracciolo et al., 2023). Here, we present new S data for the same groundmass  
83 glass (n=889) and plagioclase-, olivine- and clinopyroxene-hosted melt inclusions (MIs) (n=416) dataset  
84 published in Caracciolo et al. (2023). Sulfur was analysed by electron microprobe analyser (EMPA) at  
85 the University of Iceland using the same analytical settings as in Caracciolo *et al.* (2020) and MI  
86 compositions have been corrected for post-entrapment processes (PEP) (Caracciolo et al. 2023).

87 In this work we make use of the 'petrological method' (Devine et al., 1984) to calculate eruptive sulfur  
88 emissions by comparing the difference of S concentrations in mineral-hosted MIs with S concentrations  
89 measured in groundmass glass. The idea behind this reconstruction method is that melt inclusions  
90 preserve volatile concentrations at the time of trapping, namely the pre-eruptive volatile content,  
91 whereas quenched groundmass glasses provide an estimate of the post-eruptive volatile content. For  
92 the different magmatic units, the highest S concentration measured in PEC-corrected MIs ( $S_{MI}$ ) is  
93 selected as the pre-eruptive S concentration, whereas the lowest measurement in groundmass glasses  
94 ( $S_{glass}$ ) is chosen as post-eruptive S concentration. By combining the volume of erupted magmas with  
95  $\Delta S_{pre}$  [ $\Delta S_{pre}$  (ppm) =  $S_{MI} - S_{glass}$ ], we can assess the syn-eruptive SO<sub>2</sub> emission ( $\Delta S_{syn}$ , Mt) of individual  
96 eruptions (e.g., Bali *et al.*, 2018; Hartley *et al.*, 2018}. Furthermore, we calculate the SO<sub>2</sub> emission  
97 potential ( $\Delta S_{pot}$ , Mt), which refers to complete degassing of all pre-eruptive sulfur and reflects the  
98 maximum amount of SO<sub>2</sub> that a specific eruption could potentially have released. This reconstruction

99 method has been showed to have matched field-based volatile measurements exceptionally well  
100 during the 2014-15 Holuhraun eruption (Bali et al., 2018; Pfeffer et al., 2018) and the 2021 AD  
101 Fagradalsfjall eruption (this work, Table 1).

102

## 103 Sulfur concentrations in MI and groundmass glass

104 Sulfur concentrations in MIs are in the range 200-1900 ppm, with a relatively large variability of S at a  
105 given MI Mg#. Particularly, the most primitive MIs (Mg#>65), exclusively preserved in Reykjanes and  
106 Krýsuvík, record S contents in the range 580-1070 ppm (Fig. 1). Sulfur concentration in PEP-corrected  
107 MI compositions increases with decreasing MI Mg#, as expected for melt compositions controlled by  
108 fractional crystallization. Groundmass glasses with Mg# similar to the most evolved MIs have mean S  
109 contents varying between 150-450 ppm (Table 1). Groundmass glasses from Brennisteinsfjöll have  
110 mean S contents in the range 150-280 ppm, lower than mean S contents measured in glasses from the  
111 other volcanic systems (280-450 ppm) (Fig. 1a-d, Table 1). Sulfide globules were not observed in the  
112 erupted samples, neither within MIs nor as a stand-alone phase in the groundmass glass. For  
113 comparison, MIs from the 2021 AD Fagradalsfjall eruption contain maximum S concentrations of 1200  
114 ppm, whereas the groundmass glasses contain 20-200 ppm S, significantly less than S concentrations  
115 preserved in MIs and groundmass glasses from the 800-1240 AD Fires (Fig. 1a-d).

## 116 Assessing sulfur variability and degassing during the 800-1240 AD

### 117 Fires

118 Considering that historical eruptions on the Reykjanes Peninsula are likely sourced from mantle-  
119 derived melts of highly diverse compositions (Caracciolo et al., 2023; Harðardóttir et al., 2022;  
120 Halldórsson et al., 2022; Peate et al., 2009), including melts with variable sulfur contents (Ranta *et al.*,  
121 2022), we use our MI record to estimate S contents of the local enriched and depleted end-member  
122 melt components. We distinguish between these components from the K<sub>2</sub>O/TiO<sub>2</sub> variability, which has  
123 been proved to be a robust tracer of mantle heterogeneities in Iceland and on the RP (Halldórsson et  
124 al., 2022; Harðardóttir et al., 2022) (see supplementary information). Starting from estimated end-  
125 member melt compositions and considering that sulfur behaves as an incompatible element in basaltic  
126 magmas, most of the MI sulfur variability in our dataset can be explained by fractional crystallization  
127 (FC) and mixing of at least two end-member melt compositions (Fig. 1a-d).

128 In order to evaluate S saturation during magma ascent and fractional crystallization through the crust,  
129 we calculate sulfur content at sulfide saturation (SCSS) along a FC path, which reflects the amount of  
130 S<sup>2-</sup> present in a melt in equilibrium with a sulfide phase (Smythe et al., 2017) (see supplementary

131 information). Our modelling suggests that melts are sulfide undersaturated during most of magmatic  
132 fractionation across the RP (Fig. 1). Only magmas from Svartsengi and Brennisteinsfjöll have a high  
133 likelihood to be sulfide saturated prior to eruptions (Fig. 1). Furthermore, sulfide saturation is reached  
134 earlier during magmatic differentiation of enriched mantle-derived melts than depleted melts. That is,  
135 magmatic differentiation of the depleted and enriched end-member melts leads to sulfide saturation  
136 at  $Mg\# < 50$  and  $\sim 55-60$ , respectively.

137 Modelling of sulfur degassing with Sulfur\_X (Ding et al. 2023) suggest that basaltic melts erupted  
138 during the 800-1240 AD Reykjanes Fires are unlikely to degas significant amounts of sulfur at known  
139 pre-eruptive magma storage depths (Caracciolo et al. 2023) and that S degassing only takes place  
140 during magma ascent in the last 0.2 kbar ( $< 700$  m) (Fig. S1).

## 141 Sulfur emissions across the RP

142 Sulfur release ranges between 1000-1800 ppm across the RP, a typical range for Icelandic rift basalts  
143 (Ranta et al. 2022), with the largest  $\Delta S$  found in lava flows from Svartsengi (SÖ lavas) and  
144 Hvammahraun (h128, Brennisteinsfjöll) (Table 1).  $\Delta S$  values can be scaled by the mass of erupted  
145 material to estimate  $\Delta S_{syn}$  of individual eruptions, using published volumes of individual eruptive units  
146 emplaced during the 800-1240 AD Fires (Table 1). In this case, lava flow volumes range between 0.02  
147  $km^3$  to 0.72  $km^3$  (Einarsson et al., 1991; Jónsson, 1978; Sigurgeirsson, 2004). Using a melt density of  
148 2700  $kg/m^3$  estimated with densityX program (Iacovino and Till, 2019), we calculate  $\Delta S_{syn}$  between  
149 0.004-7 Mt (Fig. 2a). The voluminous Arnarseturshraun (SÖ-A, 0.55  $km^3$ ) and Eldvarpahraun lava flows  
150 (SÖ-E, 0.28  $km^3$ ) in Svartsengi and Hvammahraun (h128, 0.72  $km^3$ ) and Tvíbollahraun (TV, 0.37  $km^2$ )  
151 lava flows in Brennisteinsfjöll released the highest amount of  $SO_2$  into the atmosphere during the 800-  
152 1240 AD Fires. The syn-eruptive  $SO_2$  released by these latter voluminous lavas is approximately 2 to 7  
153 times larger than syn-eruptive  $SO_2$  emissions during the 2021 AD Fagradalsfjall eruption, for which we  
154 estimated  $\Delta S_{syn} = 0.93$  Mt ( $\Delta S_{measured} = 0.97 \pm 0.5$ , Barsotti et al. 2023). These are roughly between 20 to  
155 70 % of the syn-eruptive  $SO_2$  emissions estimated for the 2014-15 Holuhraun eruption ( $\Delta S_{syn} = 10.5$  Mt,  
156 Bali et al. 2018).

157 Similarly, we have calculated  $\Delta S_{pot}$ , the maximum amount of  $SO_2$  that could potentially have been  
158 released during the 800-1240 AD Fires, assuming complete degassing of  $S_{MI}$ .  $\Delta S_{pot}$  ranges between  
159 0.004-7.4 Mt and is only slightly higher than  $\Delta S_{syn}$ , as most of the sulfur is released into the atmosphere  
160 during eruptions on the RP rather than staying dissolved in the lava (Table 1).

161

162 Evaluating end-member scenarios of sulfur emissions and hazard  
163 potential for future eruptions across the RP.

164 Based on the MI record of the 2021 AD Fagradalsfjall eruption (Halldórsson et al., 2022) and the 800-  
165 1240 AD Fires (this work), we constrain maximum (1900 ppm) and minimum (1200 ppm) SO<sub>2</sub> emission  
166 potentials and use these to evaluate SO<sub>2</sub> emissions of future eruptions in the RP. With these  
167 constraints, we developed an empirical approach to assess  $\Delta S_{\text{pot}}$  for a given eruption of known lava  
168 volume, with important applications for forecasting the worst- and best-case scenarios of  $\Delta S_{\text{pot}}$  of  
169 future eruptive events (Fig. 2b). For example, based on our approach, an eruption with an eruptive  
170 volume of 0.4 km<sup>3</sup>, has the potential to release a maximum and minimum of 4.1 Mt and 2.9 Mt SO<sub>2</sub>,  
171 respectively. This method also has an application when it comes evaluating the long-term SO<sub>2</sub> impact  
172 of ongoing eruptions in the RP. If the mean magma effusion rate is known and fixed, one can roughly  
173 estimate the volume of the lava flow and calculate  $\Delta S_{\text{pot}}$  at any given moment from the onset of the  
174 eruption. During an ongoing event, this can be a valuable tool to evaluate best- and worst-case  
175 scenarios for S pollution.

176 Eruptive S emission calculations are strongly dependent on lava flow volumes. Hence, when it comes  
177 to comparing the 800-1240 AD Fires with 2021 AD Fagradalsfjall eruption, a more relevant parameter  
178 is the mean daily SO<sub>2</sub> emissions, which also is an important parameter from a hazard perspective. First,  
179 we have estimated eruption durations for the 800-1240 AD Fires starting from published erupted  
180 volumes and using mean magma output rates (MOR) calculated by Oskarsson et al. (under review), in  
181 the range 1-66 m<sup>3</sup>/s (Table 1). This yields eruption durations in the range 6 to 177 days. Secondly, we  
182 make use of inferred eruption durations to calculate daily SO<sub>2</sub> emissions and speculate about potential  
183 daily S releases during future eruptive scenarios. Daily SO<sub>2</sub> emissions during the 800-1240 AD Fires  
184 likely ranged between 600 ton/day to 53000 ton/day (Fig. 2c). In comparison, during the 2021 AD  
185 Fagradalsfjall eruption, if we assume a total amount of SO<sub>2</sub> equal to 0.97 ± 0.5 Mt (Barsotti et al.,  
186 2023), we calculate average daily SO<sub>2</sub> emissions of 5240 ± 2700 ton/day. This estimate is in agreement  
187 with the majority of measured daily SO<sub>2</sub> emissions throughout the 2021 AD Fagradalsfjall eruption, in  
188 the range 1000-7600 ton/day (Esse et al., 2023). Hence, future eruptions in the RP have the potential  
189 to release significantly more SO<sub>2</sub> on a daily basis than the 2021 AD Fagradalsfjall eruption.

190 SO<sub>2</sub> emissions during the 800-1240 AD Fires and 2021 AD Fagradalsfjall are small compared to those  
191 during the recent basaltic eruption of Holuhraun (9.2 Mt SO<sub>2</sub>, Pfeffer *et al.*, 2018). However, volcanic  
192 eruptions from the RP are potentially considered to be more hazardous due to their proximity to  
193 inhabited areas, to the international airport and to the large number of visitors expected at eruption  
194 sites (Fig. 3) (Barsotti et al. 2023). To assess the health hazard for potential future eruptions, we built  
195 seasonal wind roses, for the period 2012-2022, reflecting dominant wind speeds and directions in the

196 RP. We find that most of the time the winds blow in a direction spanning from the NW to the NE,  
197 suggesting different SO<sub>2</sub> health hazards potential associated with eruptions within different volcanic  
198 systems. Eruptions in Brennisteinsfjöll are the most hazardous, especially in spring and autumn  
199 seasons, as SO<sub>2</sub> is likely to be blown towards the capital area. Eruptions in Reykjanes pose minimal  
200 hazard as winds tend to blow away from inhabited areas. During assessment of possible eruptive  
201 scenarios in the RP, our estimates can be key input parameters to model the release and dispersion  
202 of volcanic SO<sub>2</sub> into the atmosphere. Our results can be used to inform SO<sub>2</sub> pollution hazard  
203 assessments for potential eruptive scenarios and prompt action and mitigation plans during ongoing  
204 volcanic crises in the RP.

205  
206  
207

## 208 **Acknowledgement**

209 This research was financially support by a NordVulk fellowship awarded to AC and by the Icelandic  
210 Research Fund, grant number 228933-052. We acknowledge support from the Gosvá project, a  
211 national collaborative research programme on the assessment of volcanic hazard risks in Iceland led  
212 by the Icelandic Meteorological Office (IMO) <https://en.vedur.is/about-imo/news/nr/2280>.

213  
214  
215  
216

217 **Table 1.** Eruptive units studied in this work and summary of main results.  $S_{MI}$  = pre-eruptive S  
218 concentration.  $S_{glass}$  = post-eruptive S concentration.  $\Delta S$  = sulfur emissions emitted at the vent.  $\Delta S_{syn}$  =  
219 Syn-eruptive SO<sub>2</sub> emissions.  $\Delta S_{pot}$  = SO<sub>2</sub> emission potential. Eruption durations and daily SO<sub>2</sub> emissions  
220 are calculated assuming a bulk effusion rate of 9.5 m<sup>3</sup>/s, as observed during the 2021 Fagradalsfjall  
221 eruption (Pedersen et al. 2022). <sup>a</sup> Calculations for the 2021 AD Fagradalsfjall eruption are from this  
222 work and based on MI and glass data from Halldórsson et al. 2022. Estimated  $\Delta S_{syn}$  of 0.93 Mt from  
223 this work is in agreement with measured total SO<sub>2</sub> emissions of 0.97 ± 0.5 Mt (Barsotti et al. 2023). <sup>b</sup> To  
224 our knowledge, volumes for Hrótafellshraun (HRF), Svartihryggur (h142), Húsfellsbruni (Hú1 & Hú2)  
225 and Kristnitökuhraun (KRT) lava flows are not available in the literature. We estimated the volumes of  
226 those lava flows by multiplying their area by an average thickness of 5 m, consistent with average  
227 thicknesses of lava flows of known volumes with a similar aerial extent. <sup>c</sup> MOR data are from Óskarsson  
228 et al. (under review). MOR for the 2021 Fagradalsfjall eruption is from Pedersen et al. (2022).  
229

230 **Fig. 1.** (a-d) Variation of S contents in groundmass glasses (filled circles) and PEC-corrected MIs (filled  
231 triangles) as a function of Mg# [ $Mg\# = 100 \cdot Mg / (Mg + Fe^{2+})$ ,  $Fe^{2+} / Fe^{tot} = 0.9$ ] in samples from the 800-  
232 1240 AD Fires. Data from the 2021 AD Fagradalsfjall eruption are from Halldórsson et al. (2022). Red  
233 and blue solid lines indicate fractional crystallization paths calculated for a geochemically enriched and  
234 depleted initial melt compositions, respectively (see supplementary text). The black dotted curve  
235 indicates SCSS along an empirical fractional crystallization path calculated after Smythe et al., (2017).  
236 Data are grouped in different panels according to the volcanic system and coloured according to the  
237 lava unit. (e-h) Measured MI S contents vs calculated SCSS, coloured after MgO content. SCSS was

238 calculated assuming  $Fe^{3+}/Fe_{tot} = 0.1$ ,  $P = 2$  kbar,  $T=1220$  °C and sulfide  $Fe/(Fe+Ni+Cu) = 0.65$ , after the  
239 method of Smythe et al., (2017) (cf. Fig. S3). All SCSS models were implemented in PySulfSat code  
240 (Wieser and Gleeson, 2022).  
241

242 **Fig. 2.** (a) West to east variation of  $\Delta S_{syn}$  calculated for the different eruptive units. (b)  $\Delta S_{pot}$  as a function  
243 of eruption volume for the 800-1240 AD Fires and 2021 Fagradalsfjall eruption. At a given volume,  
244 straight lines allow to calculate  $\Delta S_{pot}$  corresponding to maximum (1900 ppm) and minimum (1200 ppm)  
245  $S_{MI}$  values measured across the RP. Inset plot show most common  $\Delta S_{pot}$  across the RP, in the range 0-2  
246 Mt and for lava volumes between 0-0.3 km<sup>3</sup> (c) Maximum and minimum daily SO<sub>2</sub> emissions calculated  
247 for each volcanic system during the 800-1240 AD Fires and for the 2021 AD Fagradalsfjall (see text for  
248 calculation details). Blue kernel density estimate curve indicate measured SO<sub>2</sub> emission rates during  
249 the 2021 AD Fagradalsfjall eruption (Esse et al., 2023). Labels indicate acronyms used for the different  
250 eruptive units (c.f. Table 1).  
251

252 **Fig. 3.** Simplified geological map of the Reykjanes Peninsula and lava flows emplaced during the 800 –  
253 1240 AD Fires. The map also illustrates the aerial extent of the 2021 (Pedersen et al., 2022), 2022  
254 (Gunnarson et al., 2023) and 2023 AD (Belart et al. 2023) Fagradalsfjall lavas. The lava flows are  
255 colored according to calculated syn-eruptive SO<sub>2</sub> emissions, ranging from 0.1 to 7 Mt. Filled, white  
256 circles indicate the location of main urban areas in the Reykjanes Peninsula. Geological data are from  
257 Iceland GeoSurvey (ÍSOR) (Sæmundsson et al., 2016). Seasonal wind roses reflect data at 900 mPa  
258 (~1000 m a.s.l), which is the most common SO<sub>2</sub> injection altitude throughout the 2021 Fagradalsfjall  
259 eruption (Esse et al. 2023). Spokes indicate the direction the wind is blowing from, and the length of  
260 each spoke shows the frequency. Wind data were extracted from ERA5 (Hersbach et al. 2023).  
261

## 262 References

- 263 Bali, E., Hartley, M.E., Halldórsson, S.A., Gudfinnsson, G.H., Jakobsson, S., 2018. Melt inclusion  
264 constraints on volatile systematics and degassing history of the 2014–2015 Holuhraun  
265 eruption, Iceland. Contributions to Mineralogy and Petrology 173, 9.  
266 <https://doi.org/10.1007/s00410-017-1435-0>
- 267 Barsotti, S., Parks, M.M., Pfeffer, M.A., Óladóttir, B.A., Barnie, T., Titos, M.M., Jónsdóttir, K.,  
268 Pedersen, G.B.M., Hjartardóttir, R., Stefansdóttir, G., Johannsson, T., Arason, Gudmundsson,  
269 M.T., Oddsson, B., Prastarson, R.H., Ófeigsson, B.G., Vogfjörð, K., Geirsson, H., Hjörvar, T., von  
270 Löwis, S., Petersen, G.N., Sigurðsson, E.M., 2023. The eruption in Fagradalsfjall (2021, Iceland):  
271 how the operational monitoring and the volcanic hazard assessment contributed to its safe  
272 access. Natural Hazards. <https://doi.org/10.1007/s11069-022-05798-7>
- 273 Belart, J.M.C., Pinel, V., Reynolds, H.I., Berthier, E., Gunnarson, S.R., 2023. Digital Elevation Models  
274 (DEMs) and lava outlines from the 2023 Litla-Hrútur eruption, Iceland, from Pléiades satellite  
275 stereoimages. <https://doi.org/10.5281/zenodo.10133203>
- 276 Caracciolo, A., Bali, E., Guðfinnsson, G.H., Kahl, M., Halldórsson, S.A., Hartley, M.E., Gunnarsson, H.,  
277 2020. Temporal evolution of magma and crystal mush storage conditions in the Bárðarbunga-

278        Veiðivötn volcanic system, Iceland. *Lithos* 352–353.  
279        <https://doi.org/10.1016/j.lithos.2019.105234>

280 Caracciolo, A., Bali, E., Halldórsson, S.A., Gudfinnsson, G.H., Kahl, M., Þórðardóttir, I., Pálmadóttir,  
281        G.L., Silvestri, V., 2023. Magma plumbing systems and timescale of magmatic processes during  
282        historical magmatism on Reykjanes Peninsula. *Earth and Planetary Science Letters* 621, 118378.  
283        <https://doi.org/10.1016/j.epsl.2023.118378>

284 Carlsen, H.K., Valdimarsdóttir, U., Briem, H., Dominici, F., Finnbjörnsdóttir, R.G., Jóhannsson, T.,  
285        Aspelund, T., Gíslason, T., Gudnason, T., 2021. Severe volcanic SO<sub>2</sub> exposure and respiratory  
286        morbidity in the Icelandic population – a register study. *Environmental Health: A Global Access*  
287        *Science Source* 20, 1–12. <https://doi.org/10.1186/s12940-021-00698-y>

288 Devine, D., Sigurdsson, H., Davis, A.N., 1984. Estimates of sulfur and chlorine yield to the  
289        atmosphere from volcanic eruptions and potential climatic effects. *Journal of Geophysical*  
290        *Research* 89, 6309–6325.

291 Ding, S., Plank, T., Wallace, P.J., Rasmussen, D.J., 2023. Sulfur\_X: A Model of Sulfur Degassing During  
292        Magma Ascent. *Geochemistry, Geophysics, Geosystems* 24.  
293        <https://doi.org/10.1029/2022GC010552>

294 Einarsson, P., Eyjólfsson, V., Rut, Á., 2023. Tectonic framework and fault structures in the  
295        Fagradalsfjall segment of the Reykjanes Peninsula Oblique Rift , Iceland. *Bulletin of Volcanology*  
296        1–17. <https://doi.org/10.1007/s00445-022-01624-x>

297 Einarsson, S., Johannesson, H., Sveinbjörnsdóttir, A.E., 1991. Krísuvíkureldar II. Kapelluhraun og  
298        gátan um aldur Hellnahrauns. *Jökull* 41.

299 Esse, B., Burton, M., Hayer, C., Pfeffer, M.A., Barsotti, S., Theys, N., Barnie, T., Titos, M., 2023.  
300        Satellite derived SO<sub>2</sub> emissions from the relatively low-intensity, effusive 2021 eruption of  
301        Fagradalsfjall, Iceland. *Earth and Planetary Science Letters* 619, 118325.  
302        <https://doi.org/10.1016/j.epsl.2023.118325>

303 Fortin, M.A., Riddle, J., Desjardins-Langlais, Y., Baker, D.R., 2015. The effect of water on the sulfur  
304        concentration at sulfide saturation (SCSS) in natural melts. *Geochimica et Cosmochimica Acta*  
305        160, 100–116. <https://doi.org/10.1016/j.gca.2015.03.022>

306 Gunnarson, S.R., Belart, J.M.C., Óskarsson, B. V., Gudmundsson, M.T., Högnadóttir, T., Pedersen,  
307        G.B.M., Dürig, T., Pinel, V., 2023. Automated processing of aerial imagery for geohazards  
308        monitoring: Results from Fagradalsfjall eruption, SW Iceland, August 2022 [WWW Document].  
309        Zenodo. <https://doi.org/10.5281/ZENODO.7871187>

310 Halldórsson, S.A., Marshall, E.W., Caracciolo, A., Matthews, S., Bali, E., Rasmussen, M.B., Ranta, E.,  
311        Robin, J.G., Gudfinnsson, G.H., Sigmarsson, O., Maclennan, J., Jackson, M.G., Whitehouse, M.J.,

312 Jeon, H., van der Meer, Q.H.A., Mibei, G.K., Kalliokoski, M.H., Repczynska, M.M., Rúnarsdóttir,  
313 R.H., Sigurðsson, G., Pfeffer, M.A., Scott, S.W., Kjartansdóttir, R., Barbara, K., Kleine, B.I.,  
314 Oppenheimer, C., Aiuppa, A., Ilyinskaya, E., Bitetto, M., Giudice, G., Stefánsson, A., 2022. Rapid  
315 shifting of a deep magmatic source at Fagradalsfjall volcano, Iceland. *Nature* 609.  
316 <https://doi.org/10.1038/s41586-022-04981-x>

317 Harðardóttir, S., Matthews, S., Halldórsson, S.A., Jackson, M.G., 2022. Spatial distribution and  
318 geochemical characterization of Icelandic mantle end-members: Implications for plume  
319 geometry and melting processes. *Chemical Geology* 604.  
320 <https://doi.org/10.1016/j.chemgeo.2022.120930>

321 Hartley, M.E., Bali, E., Maclennan, J., Neave, D.A., Halldórsson, S.A., 2018. Melt inclusion constraints  
322 on petrogenesis of the 2014–2015 Holuhraun eruption, Iceland. *Contributions to Mineralogy  
323 and Petrology* 173, 1–23. <https://doi.org/10.1007/s00410-017-1435-0>

324 Heaviside, C., Witham, C., Vardoulakis, S., 2021. Potential health impacts from sulphur dioxide and  
325 sulphate exposure in the UK resulting from an Icelandic effusive volcanic eruption. *Science of  
326 the Total Environment* 774, 145549. <https://doi.org/10.1016/j.scitotenv.2021.145549>

327 Hersbach, H., Bell, B., Berrisford, P., Biavati, G., Horányi, A., Muñoz Sabater, J., Nicolas, J., Peubey, C.,  
328 Radu, R., Rozum, I., Schepers, D., Simmons, A., Soci, C., Dee, D., Thépaut, J.-N. (2023): ERA5  
329 hourly data on pressure levels from 1940 to present. Copernicus Climate Change Service (C3S)  
330 Climate Data Store (CDS), DOI: 10.24381/cds.bd0915c6 (Accessed on 26-10-2023)

331 Iacovino, K., Till, C.B., 2019. DensityX: A program for calculating the densities of magmatic liquids up  
332 to 1,627 °C and 30 kbar. *VOLCANICA* 1–10.

333 Ilyinskaya, E., Schmidt, A., Mather, T.A., Pope, F.D., Witham, C., Baxter, P., Jóhannsson, T., Pfeffer,  
334 M., Barsotti, S., Singh, A., Sanderson, P., Bergsson, B., McCormick Kilbride, B., Donovan, A.,  
335 Peters, N., Oppenheimer, C., Edmonds, M., 2017. Understanding the environmental impacts of  
336 large fissure eruptions: Aerosol and gas emissions from the 2014–2015 Holuhraun eruption  
337 (Iceland). *Earth and Planetary Science Letters* 472, 309–322.  
338 <https://doi.org/10.1016/j.epsl.2017.05.025>

339 Jónsson, J., 1978. Jarðfræðikort af Reykjaneskaga : 1. Skýringar við jarðfræðikort 2. Jarðfræðikort.  
340 Orkustofnun.

341 Milford, C., Torres, C., Vilches, J., Gossman, A.-K., Weis, F., Suárez-Molina, D., García, O.E., Prats, N.,  
342 Barreto, A., García, R.D., Bustos, J.J., Marrero, C.L., Ramos, R., China, N., Boulesteix, T., Taquet,  
343 N., Rodríguez, S., López-Darias, J., Sicard, M., Córdoba-Jabonero, C., Cuevas, E., 2023. Impact of  
344 the 2021 La Palma volcanic eruption on air quality: Insights from a multidisciplinary approach.  
345 *Science of The Total Environment* 869, 161652.

346 <https://doi.org/10.1016/j.scitotenv.2023.161652>

347 Óskarsson, B. V. , Askew, R. A., Guðmundsson, H. (under review) The eruption capacity of effusive  
348 volcanism on the Reykjanes peninsula. *Bulletin of volcanology*

349 Peate, D.W., Baker, J.A., Jakobsson, S.P., Waight, T.E., Kent, A.J.R., Grassineau, N. V., Skovgaard, A.C.,  
350 2009. Historic magmatism on the Reykjanes Peninsula, Iceland: A snap-shot of melt generation  
351 at a ridge segment. *Contributions to Mineralogy and Petrology* 157, 359–382.

352 <https://doi.org/10.1007/s00410-008-0339-4>

353 Pedersen, G.B.M., Belart, J.M.C., Óskarsson, B.V., Gudmundsson, M.T., Gies, N., Högnadóttir, T.,  
354 Hjartadóttir, Á.R., Pinel, V., Berthier, E., Dürig, T., Reynolds, H.I., Hamilton, C.W., Valsson, G.,  
355 Einarsson, P., Ben-Yehosua, D., Gunnarsson, A., Oddsson, B., 2022. Volume, Effusion Rate, and  
356 Lava Transport During the 2021 Fagradalsfjall Eruption: Results From Near Real-Time  
357 Photogrammetric Monitoring. *Geophysical Research Letters* 49, 1–11.

358 <https://doi.org/10.1029/2021GL097125>

359 Pfeffer, M.A., Bergsson, B., Barsotti, S., Stefánsdóttir, G., Galle, B., Arellano, S., Conde, V., Donovan,  
360 A., Ilyinskaya, E., Burton, M., Aiuppa, A., Whitty, R.C.W., Simmons, I.C., Arason, P., Jónasdóttir,  
361 E.B., Keller, N.S., Yeo, R.F., Arngrímsson, H., Jóhannsson, Þ., Butwin, M.K., Askew, R.A., Dumont,  
362 S., Von Löwis, S., Ingvarsson, Þ., La Spina, A., Thomas, H., Prata, F., Grassa, F., Giudice, G.,  
363 Stefánsson, A., Marzano, F., Montopoli, M., Mereu, L., 2018. Ground-Based measurements of  
364 the 2014–2015 holuhraun volcanic cloud (Iceland). *Geosciences (Switzerland)* 8, 1–25.

365 <https://doi.org/10.3390/geosciences8010029>

366 Ranta, E., Gunnarsson-Robin, J., Halldórsson, S.A., Ono, S., Izon, G., Jackson, M.G., Reekie, C.D.J.,  
367 Jenner, F.E., Guðfinnsson, G.H., Jónsson, Ó.P., Stefánsson, A., 2022. Ancient and recycled sulfur  
368 sampled by the Iceland mantle plume. *Earth and Planetary Science Letters* 584, 117452.

369 <https://doi.org/10.1016/j.epsl.2022.117452>

370 Sæmundsson, K., Sigurgeirsson, M., Friðleifsson, G.Ó., 2020. Geology and structure of the Reykjanes  
371 volcanic system, Iceland. *Journal of Volcanology and Geothermal Research* 391, 106501.

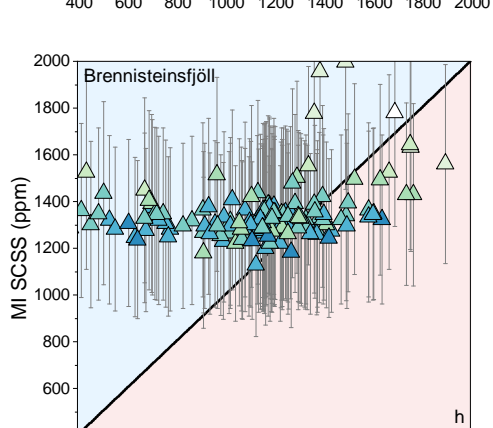
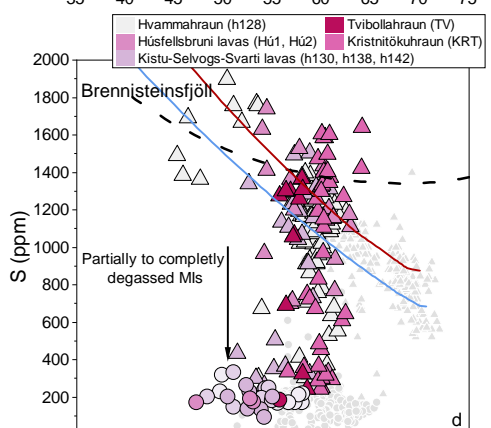
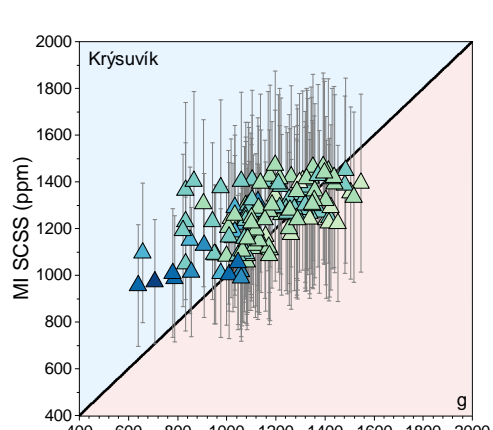
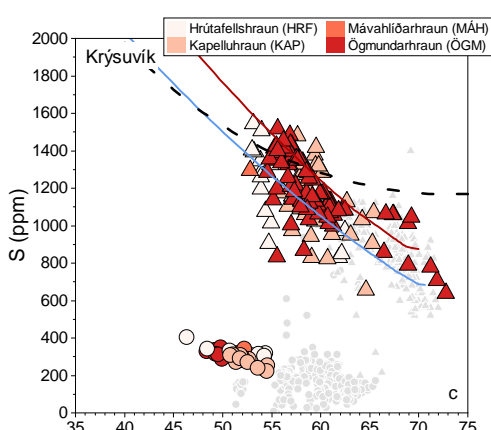
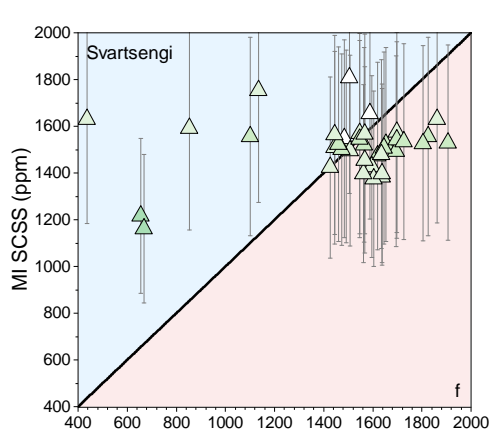
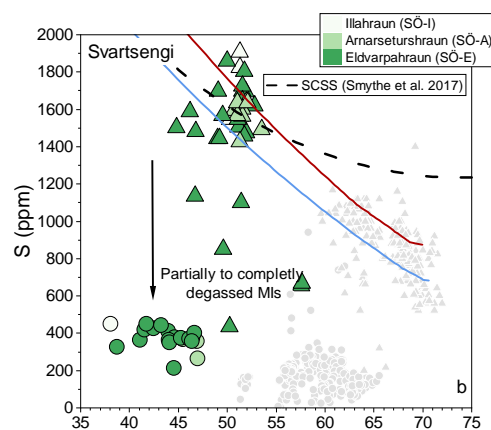
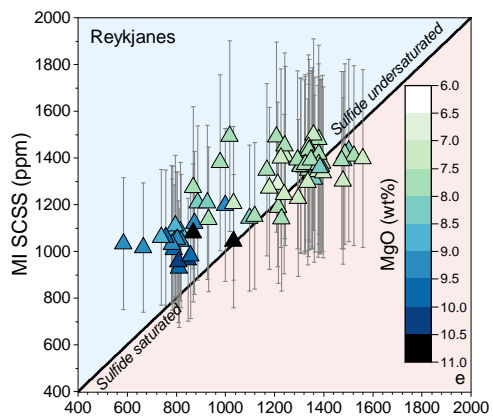
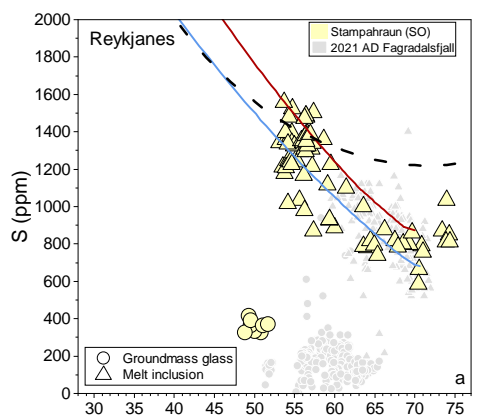
372 <https://doi.org/10.1016/j.jvolgeores.2018.11.022>

373 Sæmundsson, K., Sigurgeirsson, M.A., Hjartarson, Á., Kaldal, I., Kristinsson, S.G., 2016. Geological  
374 Map of Southwest Iceland, 1: 100 000 (2nd ed.). Reykjavik: Iceland GeoSurvey.

375 Schmidt, A., Leadbetter, S., Theys, N., Carboni, E., Witham, C.S., Stevenson, J.A., Birch, C.E.,  
376 Thordarson, T., Turnock, S., Barsotti, S., Delaney, L., Feng, W., Grainger, R.G., Hort, M.C.,  
377 Höskuldsson, Á., Ialongo, I., Ilyinskaya, E., Jóhannsson, T., Kenny, P., Mather, T.A., Richards,  
378 N.A.D., Shepherd, and J., 2015. Satellite detection, long-range transport, and air quality  
379 impacts of volcanic sulfur dioxide from the 2014–2015 flood lava eruption at Bárðarbunga

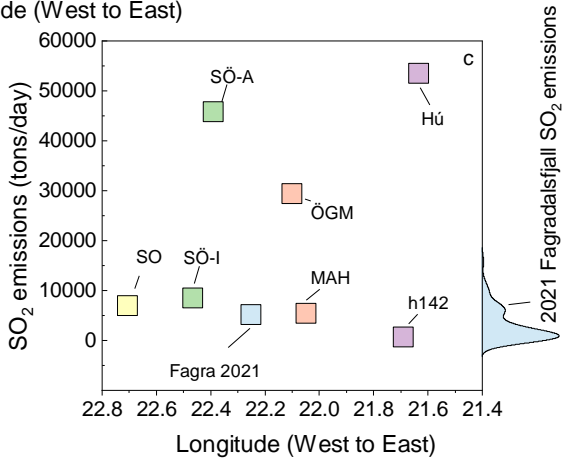
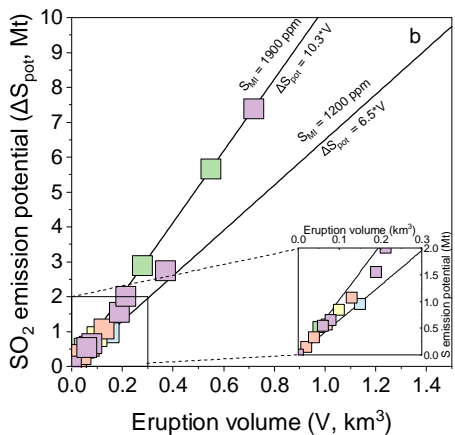
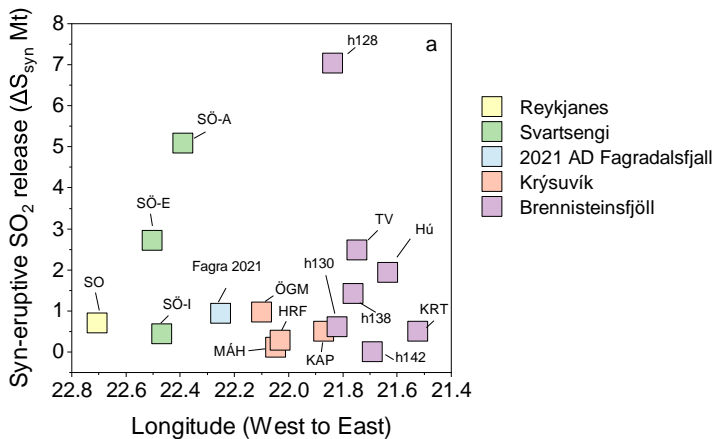
380 (Iceland). Journal of Geophysical Research: a 120, 1–17.  
381 <https://doi.org/10.1002/2014JC010485>.Received  
382 Sigurgeirsson, M.A., 2004. Þáttur úr gossögu Reykjaness. Náttúrufræðingurinn 72, 21–28.  
383 Smythe, D.J., Wood, B.J., Kiseeva, E.S., 2017. The S content of silicate melts at sulfide saturation:  
384 New experiments and a model incorporating the effects of sulfide composition. American  
385 Mineralogist 102, 795–803. <https://doi.org/10.2138/am-2017-5800CCBY>  
386 Weiser, F., Baumann, E., Jentsch, A., Medina, F.M., Lu, M., Nogales, M., Beierkuhnlein, C., 2022.  
387 Impact of Volcanic Sulfur Emissions on the Pine Forest of La Palma, Spain. Forests 13.  
388 <https://doi.org/10.3390/f13020299>  
389 Wieser, P.E., Gleeson, M., 2022. PySulfSat: An Open-Source Python3 Tool for modelling sulfide and  
390 sulfate saturation.  
391

Eruptive unit	Acronym	Volcanic system	Longitude	Glass S			S <sub>MI</sub>	S <sub>glass</sub>	ΔS	Volume	Mass	ΔS <sub>syn</sub>	ΔS <sub>pot</sub>	MOR <sup>c</sup>	Eruption duration	Daily SO <sub>2</sub>
				Mean ppm	±1σ ppm	ppm										
Stampahraun 4	SO	Reykjanes	22.70	360	50	1559	258	1301	0.1	2.7E+11	0.70	0.84	6.5	177	4745	
Arnarseturshraun	SÖ-A	Svartsengi	22.39	300	68	1907	196	1711	0.55	1.5E+12	5.08	5.66	51.5	124	45778	
Eldvarpahraun	SÖ-E	Svartsengi	22.50	390	60	1907	112	1795	0.28	7.6E+11	2.71	2.88	33.8	96	30045	
Illahraun	SÖ-I	Svartsengi	22.47	450	155	1907	312	1595	0.05	1.4E+11	0.43	0.51	6.2	93	5529	
Fagradalsfjall 2021	Fagra 2021	Fagradalsfjall	22.25	190	100	1170	20	1150	0.15	4.1E+11	0.93 <sup>a</sup>	0.95 <sup>a</sup>	9.5	185	5120	
Ögmundarhraun	ÖGM	Krýsuvík	22.10	290	50	1517	138	1379	0.13	3.5E+11	0.97	1.06	41.5	36	29345	
Kapelluhraun	KAP	Krýsuvík	21.87	280	42	1482	183	1299	0.07	1.9E+11	0.49	0.56	31.0	26	21415	
Mávahlíðarhraun	MÁH	Krýsuvík	22.05	340	30	1297	280	1017	0.02	5.4E+10	0.11	0.14	8.9	26	5362	
Hrútafellshraun <sup>b</sup>	HRF	Krýsuvík	22.03	330	50	1546	252	1294	0.04 <sup>b</sup>	1.1E+11	0.27	0.33	17.5	26	12611	
Hvammahraun	h128	Brennisteinsfjöll	21.84	190	70	1900	90	1810	0.72	1.9E+12	7.03	7.38	49.1	170	43485	
Kistuhraun	h130	Brennisteinsfjöll	21.82	210	60	1494	94	1400	0.08	2.2E+11	0.60	0.64	7.9	117	5501	
Selvogshraun	h138	Brennisteinsfjöll	21.76	180	40	1504	126	1378	0.19	5.1E+11	1.41	1.54	14.4	153	10095	
Tvibollahraun	tv	Brennisteinsfjöll	21.75	180	30	1367	129	1238	0.37	1.0E+12	2.47	2.73	36.9	116	23480	
Svartihryggur <sup>b</sup>	h142	Brennisteinsfjöll	21.69	280	150	1341	147	1194	0.0005 <sup>b</sup>	1.5E+09	0.004	0.00	1.0	6	613	
Húsfellsbruni <sup>b</sup>	Hú1 & Hú2	Brennisteinsfjöll	21.63	180	55	1739	55	1684	0.2 <sup>b</sup>	5.8E+11	1.94	2.00	65.9	25	53442	
Kristnitökuhraun <sup>b</sup>	KRT	Brennisteinsfjöll	21.52	180	40	1640	118	1522	0.06 <sup>b</sup>	1.6E+11	0.50	0.54	18.4	38	14066	

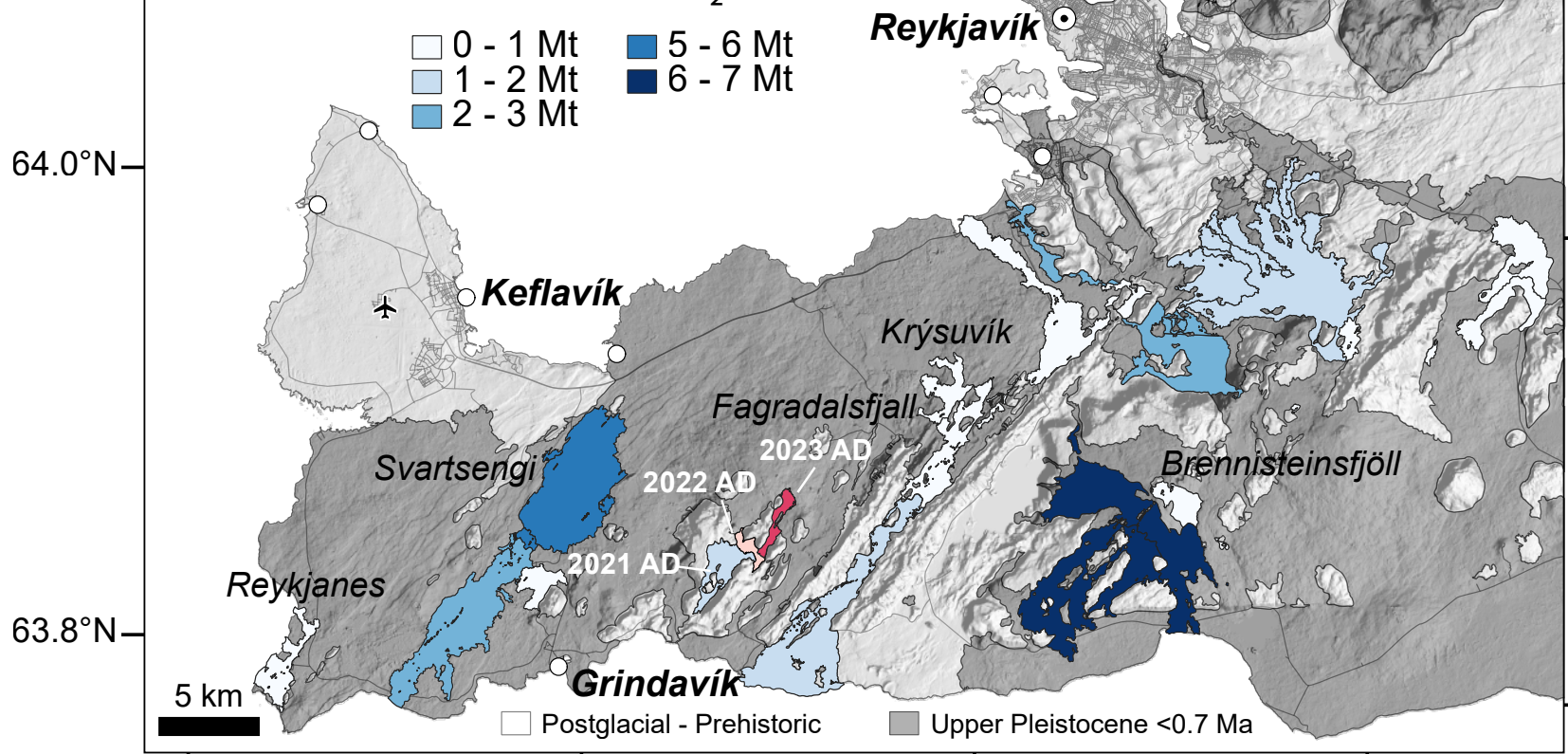


Glass or MI Mg#

MI S (ppm)



# 800-1240 AD Fires SO<sub>2</sub> release



Pressure Level 900 mbar  
Time period 2012-2022

